**Mathematical modeling**

**Математическое моделирование**

*UDC 539.3*
*https://doi.org/10.32362/2500-316X-2023-11-3-86-103*



REVIEW ARTICLE

# Mathematical modeling of experiments on the interaction of a high-power ultraviolet laser pulse with condensed targets

**Ivan G. Lebo** @

*MIREA – Russian Technological University, Moscow, 119454 Russia*
@ *Corresponding author, e-mail: lebo@mirea.ru*

**Abstract**

**Objectives.** The paper aimed to review and analyze the results of works devoted to numerical modeling of experiments on the interaction of high-power ultraviolet (UV) laser pulses with condensed targets. The experiments were carried out at GARPUN, the powerful KrF-laser facility at the P.N. Lebedev Physical Institute of the Russian Academy of Sciences (Moscow). The relevance of the research is related to the use of excimer UV lasers as a driver for a thermonuclear reactor. Physical aspects of laser–plasma interaction, including those related to the possibility of using two-sided cone target in a fission–fusion reactor, are discussed.

**Methods.** The research is based on physico-mathematical models, including Euler and Lagrange.

**Results.** The mathematical modeling of three types of natural experiments is presented: (1) burning through different thicknesses of Al foils by high-power UV laser; (2) studying hydrodynamic instability development at the UV laser acceleration of thin polymer films and features of turbulent zone formation; (3) interaction of high-power UV laser pulses with two-layer targets (Al + Plexiglas) and study of fine structures. Numerical modeling showed that a hybrid reactor with UV laser driver can use targets in the form of two-sided counter cones.

**Conclusions.** Physico-mathematical models are developed along with 2D codes in Lagrangian and Eulerian coordinates as confirmed in the results of natural experiments. The models can be used to describe the physics of high-power UV laser pulses interacting with various targets and forecast the results of reactor-scale experiments.

**Keywords:** numerical modeling, high-power UV laser pulse interaction with plasma, hybrid reactor with laser initiation

• **Submitted:** 22.06.2022 • **Revised:** 07.12.2022 • **Accepted:** 12.03.2023

**For citation:** Lebo I.G. Mathematical modeling of experiments on the interaction of a high-power ultraviolet laser pulse with condensed targets. *Russ. Technol. J*. 2023;11(3):86–103. https://doi.org/10.32362/2500-316X-2023-11-3-86-103

**Financial disclosure:** The author has no a financial or property interest in any material or method mentioned.

The author declares no conflicts of interest.

ОБЗОР

# Численное моделирование экспериментов по взаимодействию мощных ультрафиолетовых лазерных импульсов с конденсированными мишенями

**И.Г. Лебо** [@]

*МИРЭА – Российский технологический университет, Москва, 119454 Россия*
[@] *Автор для переписки, e-mail: lebo@mirea.ru*

**Резюме**

**Цели.** Цель исследования – обзор и анализ результатов работ, посвященных численному моделированию экспериментов по взаимодействию мощных ультрафиолетовых (УФ) лазерных импульсов с конденсированными мишенями. Натурные эксперименты были выполнены в Физическом институте им. П.Н. Лебедева РАН на мощном криптон-фтор (KrF) лазере «ГАРПУН». Актуальность исследований связана с тем, что эксимерные УФ-лазеры являются одним из основных претендентов на драйвер в термоядерном реакторе. Физика взаимодействия такого излучения с плазмой имеет свою специфику. Обсуждается возможность использования мишеней в виде встречных конусов в таком ядерно-термоядерном реакторе.

**Методы.** Для моделирования лазер-плазменных процессов используются физико-математические модели, лагранжевы и эйлеровы методики, двумерные программы в цилиндрических и сферических координатах.

**Результаты.** Представлены результаты численного моделирования трех типов экспериментов: а) прожигание УФ-лазером алюминиевых фольг различной толщины; б) изучение развития гидродинамической неустойчивости при ускорении тонких полимерных пленок мощным УФ-импульсом и особенностей формирования турбулентного слоя; в) взаимодействие мощных УФ-импульсов с двухслойными мишенями (алюминий + оргстекло) и исследование «тонких» структур, формирующихся в веществе. На основании численных расчетов показано, что в гибридном реакторе с УФ-лазерным драйвером могут применяться мишени в виде двухсторонних встречных конусов.

**Выводы.** Развиты физико-математические модели и апробированы двумерные программы в эйлеровых и лагранжевых координатах на натурных экспериментах, позволяющие описывать физику взаимодействия мощных УФ-лазерных импульсов с мишенями различной конструкции. Это дает возможность прогнозировать эксперименты реакторного масштаба.

**Ключевые слова:** численное моделирование, взаимодействие мощных УФ-лазеров с плазмой, гибридные реакторы с лазерным инициированием

• **Поступила:** 22.06.2022 • **Доработана:** 07.12.2022 • **Принята к опубликованию:** 12.03.2023

**Для цитирования:** Лебо И.Г. Численное моделирование экспериментов по взаимодействию мощных ультрафиолетовых лазерных импульсов с конденсированными мишенями. *Russ. Technol. J.* 2023;11(3):86–103. https://doi.org/10.32362/2500-316X-2023-11-3-86-103

**Прозрачность финансовой деятельности:** Автор не имеет финансовой заинтересованности в представленных материалах или методах.

Автор заявляет об отсутствии конфликта интересов.

## INTRODUCTION

Laser thermonuclear fusion (LTF) research has been conducted in Russia and abroad since the 1960s [1]. Using powerful laser pulses, targets containing a deuterium-tritium (DT) mixture are heated and compressed. As a result, fusion reactions occur in the compressed fuel (for more details on the physics of laser fusion, see [2, 3]). A number of important requirements are imposed on the laser ("driver"): the energy in the pulse should be equal to a few megajoules; the radiation intensity on the target surface should be $10^{15}$–$10^{16}$ W/cm$^2$ in the visible or ultraviolet wavelength range; the laser pulse of 10–100 ns duration should have a given temporal intensity "profiling"; and the target must be exposed to good uniformity to reduce instability during fuel

compression. To create a fusion reactor, along with high fusion flare efficiency (gain factor $G = E_f/E_{las} >> 1$, where $E_f$ is released fusion energy and $E_{las}$ is absorbed plasma energy of the laser pulse) requires that the driver can operate in the frequency mode (1–10 Hz) with a large resource and high efficiency ($\eta \approx 1$–10%).

In Russia [4] and abroad[1] [5–11], powerful laser facilities are being built to initiate thermonuclear microbursts and conduct research in this field of knowledge. The NIF (National Ignition Facility, Lawrence Livermore National Laboratory, USA) laser facility built for LTF purposes has been in operation since 2012. A record fusion neutron yield $Y_n = (4–5) \cdot 10^{17}$ corresponding to ≈0.7$G$ was achieved at this facility in August 2021 [6][2]. As well as NIF, facilities under construction (UFL-2M, Russian Federal Nuclear Center – All-Russian Research Institute of Experimental Physics (RFNC–VNIIEF), Russia; Laser Mégajoule[3], France; Shen Guang[4], China) are based on solid-state Nd lasers[5], which currently appear to be the most promising in terms of demonstrating single thermonuclear microbursts. However, this type of laser has serious disadvantages in terms of creating a driver for a thermonuclear reactor. While gas excimer lasers offer a number of advantages, such as functioning directly in the ultraviolet wavelength range, the ability to operate with a pulse repetition rate greater than 1 Hz, as well as a wide generation frequency bandwidth, these types of lasers also have disadvantages.

Due to the high cost (in the region of $10 bn), systematic research is required to support the right decisions when deciding to build the driver for a fission reactor. The GARPUN facility hosted at the P.N. Lebedev Physical Institute of the Russian Academy of Sciences (FIAN) serves to produce a hot dense plasma. This is based on an excimer KrF-laser with pulse energy $E_L \approx 100$ J, pulse duration $\tau = 100$ ns, and wavelength $\lambda = 0.248$ μm. For interpreting experimental data, physico-mathematical models and programs have been developed to solve problems involved in interaction of powerful laser pulses with condensed and gaseous targets, as well as predicting new LTF target designs. Below is the review of studies on the mathematical modeling of three series of experiments performed at the GARPUN facility, as well as the study of targets in the form of counter cones being promising for LTS purposes.

## BRIEF DESCRIPTION OF THE PHYSICO-MATHEMATICAL MODELS AND TWO-DIMENSIONAL PROGRAMS *ATLANT* AND *NUTCY*

The *Atlant* software package [12] consists of programs simulating the dynamics and energy transfer in laser plasma in spherical (*Atlant_Sp* version: coordinates $\check{r}$ is radius-vector module; θ, $t$ is time) and cylindrical (*Atlant_C* version: coordinates $r$, $z$, $t$ is time) geometries.

The equations describing the evolution of the laser target in the two-temperature approximation may be written as follows:

$$\frac{d\rho}{dt} = -\rho \operatorname{div} \bar{\mathbf{u}}, \tag{1}$$

$$\rho \frac{d\bar{\mathbf{u}}}{dt} = -\rho \operatorname{grad} P, \tag{2}$$

$$\left( \frac{\bar{\vartheta}}{|\vartheta|}, \nabla \right) \bar{\vartheta} = K \bar{\vartheta}, \tag{3}$$

$$\rho \frac{d\varepsilon_e}{dt} = -P_e \operatorname{div} \bar{\mathbf{u}} + \operatorname{div} W_e - Q - R_{self} + \operatorname{div} \bar{\vartheta}, \tag{4}$$

$$\rho \frac{d\varepsilon_i}{dt} = -P_i \operatorname{div} \bar{\mathbf{u}} + \operatorname{div} W_i + Q, \tag{5}$$

$$W_e = æ_e \operatorname{grad} T_e, \tag{6}$$

$$W_i = æ_i \operatorname{grad} T_i, \tag{7}$$

$$Q = Q_0 \frac{T_e - T_i}{T_e^{3/2}} \rho^2, \tag{8}$$

$$P_e = P_e(\rho, T_e), P_i = P_i(\rho, T_i), \tag{9}$$

$$\frac{dZ_i}{dt} = Z_i \cdot (\varphi_i - \varphi_r - \varphi_{fr}), \tag{10}$$

$$\varepsilon_e = \varepsilon_e(\rho, T_e), \varepsilon_i = \varepsilon_i(\rho, T_i),$$

$$R_{self} = R_{self}(\rho, T_e), P = P_i + P_e, \tag{11}$$

$$æ_e = æ_e(\rho, T_e), æ_i = æ_i(\rho, T_i), K = K(\rho, T_e), Q_0 = Q_0(\rho, T_e),$$

where $P_e$, $P_i$, $T_e$, $T_i$ are electron and ion pressures and temperatures; ρ is matter density; $\bar{\mathbf{u}}$ is the hydrodynamic velocity vector; $P$ is the total pressure; $P_e$, $P_i$ are electron and ion pressures; $\varepsilon_e$, $\varepsilon_i$ are electron and ion specific internal energies; $æ_e$, $æ_i$ are electron and ion thermal

[1] Kritcher A. and HIBRYD-E ICF team. Initial results from HYBRID-E DT experiment N210808 with >1.3 MJ yield. *IFSA Virtual Meeting*. September 2021. LLNL-PRES-826367. P. 16. https://www.aps.org/units/maspg/meetings/upload/obenschain-11172021.pdf. Accessed February 07, 2023.

[2] In December 2022, reports appeared on the Internet that $G \approx 1.5$ was obtained at the NIF facility in the United States!

[3] https://www-lmj.cea.fr/. Accessed February 07, 2023.

[4] https://lssf.cas.cn/en/facilities-view.jsp?id=ff8080814ff56599014ff5a31abb004a. Accessed February 07, 2023.

[5] The Nd-laser generates radiation in the infrared range $\lambda = 1.06$ μm, and expensive complex devices are required to convert to 2nd and 3rd harmonics.

conductivity coefficients; $\bar{\vartheta}$ is the laser radiation flux; $K$ is the absorption coefficient; $Q$ is the exchange term; $R_{self}$ is the energy sink due to the plasma self-radiation; $Z_i$ is the ion charge average in the Lagrangian cell; $\varphi_i$, $\varphi_r$, $\varphi_{fr}$ are rates of ternary ionization, ternary recombination, and photorecombination.

The pressure and zero heat flux are set at the outer boundary, while heat fluxes and zero velocity components in the direction normal to the boundary are set on the axis of rotation ($\theta = 0$ in the spherical coordinate system, $r = 0$ in the cylindrical one) and zero symmetry planes. The initial conditions can be arbitrary.

The solution of equations (1)–(11) is performed numerically using additive accounting schemes for physical processes.

The *Atlant* program suite, which has been developed during the last four decades, consists of several programs with the following features: (1) the physical model is based on the dense high-temperature laser plasma; (2) a two-dimensional Lagrangian coordinate system is used; (3) the modular principle of program writing; (4) all programs are written in FORTRAN language. More detailed information on the *Atlant* software package can be found in [12, 13].

The *NUTCY* software [12] allows solving numerically gas dynamics equations in two-dimensional cylindrical ($r$, $z$, $t$ is time) geometry in Eulerian coordinates [12]:

$$\frac{\partial \rho}{\partial t} + \frac{1}{r}\cdot\frac{\partial r\rho u}{\partial r} + \frac{\partial \rho\omega}{\partial z} = 0,$$

$$\frac{\partial \rho u}{\partial t} + \frac{1}{r}\cdot\frac{\partial r\rho u^2}{\partial r} + \frac{\partial \rho u\omega}{\partial z} + \frac{\partial \rho}{\partial r} = 0, \qquad (12)$$

$$\frac{\partial \rho\omega}{\partial t} + \frac{1}{r}\cdot\frac{\partial ru\omega}{\partial r} + \frac{\partial \rho u\omega}{\partial z} + \frac{\partial \rho}{\partial z} = 0,$$

$$\frac{\partial e}{\partial t} + \frac{1}{r}\cdot\frac{\partial ru(e+p)}{\partial r} + \frac{\partial (e+p)\omega}{\partial z} = -div\, q_T - div\, q_L.$$

Here, $\rho$ is density; $p$ is pressure; $V_r = u$, $V_z = \omega$ are components of the velocity vector $\mathbf{V}$; $e = \rho\left(\varepsilon + \frac{\mathbf{V}^2}{2}\right)$ is the total energy; $q_T = -æ_e \operatorname{grad} T$ is the flux of electronic heat conductivity; $q_L$ is the flux of laser radiation.

A one-temperature approximation is used, i.e., it is assumed that the relaxation time between the electronic and ionic components is short compared to the typical time of change in the basic thermodynamic quantities. The system of equations (12) is supplemented by the equation of state $p = (\gamma - 1)\rho\varepsilon$, where $\varepsilon$ is the specific internal energy, $\gamma$ is the adiabatic index, and the continuity equation for each gas component ($n$ components in total):

$$\frac{\partial \rho_i}{\partial t} = \operatorname{div} \rho_i \mathbf{V} = 0, \text{ where } i = \overline{1, n-1}. \qquad (13)$$

If the gas contains two components, it would be convenient to solve the continuity equation for the mixture (the upper equation of the system (12)) and then the equation for one of the components (13). Then, the first component concentration $C$ is determined, while the second component concentration is equal to $(1 - C)$.

This program also uses the modular (block) principle for writing the program using the FORTRAN programming language.

For solving equations (12), (13), total variation diminishing differential schemes of increased approximation order (gas dynamics block) and implicit schemes for taking into account electronic thermal conductivity are used [13]. Methods for solving such problems have been developed at the Institute of Mathematical Modeling and the Keldysh Institute of Applied Mathematics of the Russian Academy of Sciences [12, 14, and 15] with direct participation of the author.

## MODELING EXPERIMENTS ON BURNING FOIL

Experiments on burning through aluminum foils were carried out at the GARPUN facility [16]. The intensity of the radiation incident on the target was $I \approx 6 \cdot 10^{12}$ W/cm$^2$, while the plasma interaction efficiency parameter $(I \cdot \lambda^2) \approx 3.4 \cdot 10^{13}$ (W/cm$^2$)·μm$^2$.

At fixed parameters of incident laser flux on the aluminum foil (target), the thickness of this foil is varied. After placing a screen behind the foil, the time delay between the appearance of glow on the screen and the time of the appearance of plasma glow on the front surface of the target is measured (Fig. 1).

In the experiments, burning through aluminum foils down to 300 μm is observed during the laser pulse duration.

Figure 2a shows the temporal shape of the laser pulse and compares the results of numerical calculations performed using the *NUTCY* program (solid curves) with experimental data (vertical red bars). The yellow curve shows quasi-dimensional calculations (when the distribution of radiation intensity in the transverse direction is set as a constant value). The blue line shows the results of fully two-dimensional calculations where the intensity is set in the following way: $I(r, t) = I_1(t) \cdot I_r(r)$ with the transverse intensity distribution having the form $I_r = C_0/\exp(r/R_f)^2$. Here, $C_0$ is the normalization constant such that $2\pi\int_0^{R_0} I_r r dr = 1$, $R_0$ is the transverse radius of the calculated region, $R_f = 49$ μm. In both variants, the laser intensity averaged over the focusing spot is the

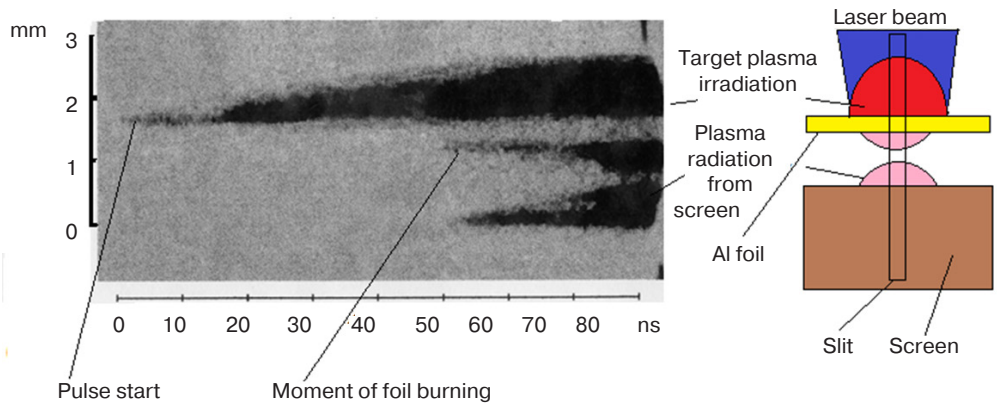


**Fig. 1.** Plasma glow obtained through a slit using the photoelectronic recorder as a function of time (left); scheme of the experiment (right) [12]

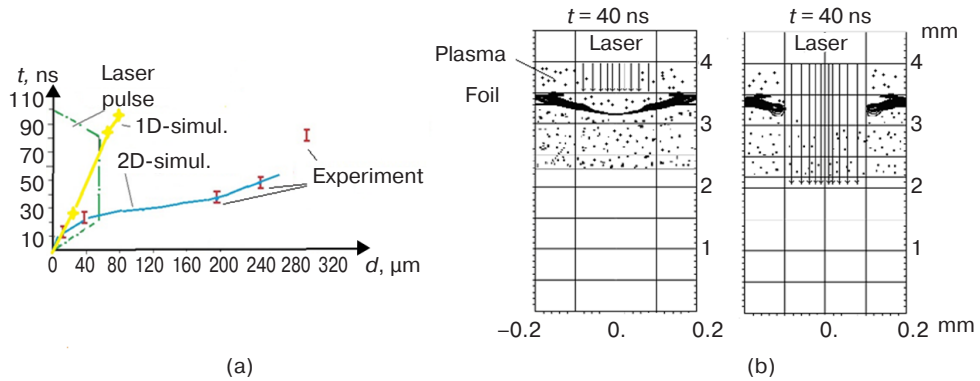


**Fig. 2.** Laser pulse time shape and the results of one-dimensional (1D) and two-dimensional (2D) calculations and experimental data (a); density isolines at time moments $t$ = 40 ns (up to the moment of foil burning through) and $t$ = 45 ns (moment of burning through) (b) [12]

same. $I_1$ is time dependence of the laser pulse, which has a trapezoid shape with time moments at tops $t_1$ = 0 ns, $t_2$ = 20 ns, $t_3$ = 80 ns, and $t_4$ = 100 ns. $\int_0^\infty I_1(t)dt = E_{las}$ is absorbed laser energy.

The foil density isolines are shown in Fig. 2b. In this calculation, the initial thickness of the aluminum foil is 200 μm (initial density ρ = 2.7 g/cm$^3$).

Figure 2a shows good agreement between two-dimensional calculations and the experimental data on the "penetration time", but a significant discrepancy with the results of one-dimensional calculations. Along with the evaporation of outer layers towards the incident radiation (directly connected with the burning-through process), the most likely explanation for this is the effect of diverging cone-shaped shock waves (SWs) formed near the crater apex, which plays an important role in such foil "drilling". These "move apart" cold dense layers to increase the penetration depth of laser radiation [16].

In this case, the distance $L_{SW}$ that the SW travels during the laser pulse duration (SW velocity $V_{SW} \sim 5$ km/s, $t \sim 100$ ns, then $L_{SW} \sim 500$ μm) is much larger than the focus spot size ($2R_f \approx 100$ μm).

## MODELING EXPERIMENTS ON TURBULENT LAYER DEVELOPMENT DURING LASER ACCELERATION OF THIN FILMS

The Richtmyer–Meshkov instability that develops when SWs pass through the contact surfaces of two gases or plasma results in the rapid evolution of initially small perturbations of interface surface of two media to the formation and the development of a turbulent layer [17, 18]. Studying the laws of turbulence development in the physics of extreme state of matter is an extremely important task in inertial thermonuclear fusion in cosmology and astrophysics [2].

Using powerful laser pulses, it is possible to accelerate dense unevaporated layers to velocities of ~10–100 km/s. It has been proposed to accelerate such layers in special transparent cells filled with a gas or two gases separated by a thin film. The development features of hydrodynamic instabilities of the contact boundary perturbations and transition into the turbulent state may be studied in such "laser shock tubes" [19].

In the second series of experiments, the development of the turbulent layer during laser acceleration of thin Lavsan™ films with a thickness of 1–50 μm is studied

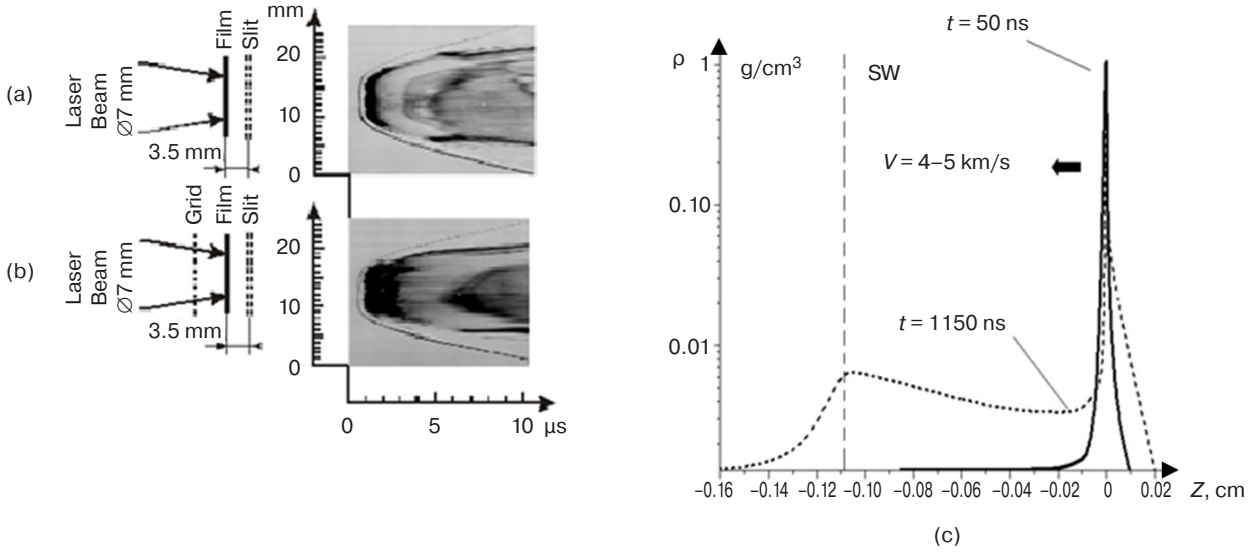


**Fig. 3.** Schematic of experiments (left) and images of the accelerated layer obtained with slit sweep in the case of uniform (a) and nonuniform (b) irradiation, ∅ is a side of a square-shaped laser beam; numerical calculation results of the density distribution along the *OZ* axis at time moments $t$ = 50 ns and $t$ = 1150 ns (c) [20]

at the GARPUN facility. The targets are placed inside a vacuum chamber filled with air or argon with initial pressure of 0.0002–1.0 bar. Laser radiation is focused into the 7 × 7 mm$^2$ square spot using a prism raster, thus ensuring irradiation uniformity not worse than 1–2%. The intensity of laser radiation on the target surface is varied $I$ = 0.1–1.0 GW/cm$^2$ by attenuating the power of the incident light beam. The slit of the electron photochronograph is parallel to the film surface and is located at different distances behind it. The "registograms" of a film with initial thickness $d$ = 5 μm irradiated by laser with intensity $I$ = 0.55–0.65 GW/cm$^2$ in the air at atmospheric pressure are shown in Figs. 3a and 3b. The slit is placed at the distance of 3.5 mm behind the initial position of the film. In Fig. 3a, homogeneous radiation falls on the target surface, while in Fig. 3b, the radiation passes through the wire mesh with a mesh size of 0.7 × 0.7 mm$^2$ placed in front of the film at the distance of ~1 cm. This provides a given scale of the intensity nonuniformity. In the second case, the thickness of the dense layer flying past the slit is 3–4 times greater than in the first case. The density profiles obtained in numerical calculations at time moments $t$ = 50 ns and $t$ = 1150 ns are shown in Fig. 3c. The density maxima are combined in one point for easy comparison. The vertical dashed line is the shock front at time moment $t$ = 1150 ns.

The process of laser acceleration of the film is simulated using the cylindrical version of the *Atlant* software package. It is shown that numerical calculations accurately reproduce the dynamics of the film flight. The velocity is ~3–4 km/s at the moment when the dense layer flies past the slit.[6] The initial density of the film is 1 g/cm$^3$. During flight, the layer density should be noted to decrease with time due to thermal expansion, as well as due to the purely geometrical factor of increasing the surface of the layer boundary. By the moment $t$ = 1150 ns (when the layer reaches a distance of 3.5 mm from the initial position), the density maximum is 0.1 g/cm$^3$. By this point, the width of the dense layer has increased compared to the initial one (Fig. 3c). The development of turbulent mixing during laser acceleration and braking of the layer by the surrounding air results in an additional increase in the film thickness. Thus, at a layer flight velocity of ~3 km/s and time of flight past the slit of ~0.5 μs, the layer width is 1.5 mm, while in the calculation with no allowance for turbulent mixing, it is an order of magnitude smaller (Fig. 3c). In the experiments with the perturbed laser flux (Fig. 3b), the layer thickness is 3–5 times greater.

For modeling turbulence, the turbulent mixing model described in [21, 22] is used. In this model it is assumed that the turbulent layer develops according to the laws of diffusion, but with empirical coefficients obtained from natural experiments. Thus, the turbulent diffusion equation may be written as follows:

$$\frac{\partial \rho}{\partial t} = \frac{\partial}{\partial z}\left( D_m \frac{\partial \rho}{\partial z} \right), \qquad (14)$$

where ρ is density and $D_m$ is the turbulent mixing coefficient,

$$D_m = l_\rho^2 \omega_t, \; \omega_t = \left( \frac{\partial \ln \rho}{\partial z} \cdot \frac{1}{\rho} \cdot \frac{\partial P}{\partial z} \right)^{0.5}. \qquad (15)$$

[6] By the time $t$ = 50 ns, the boundary of the air–CH layer accelerated to 4–5 m/s. Then the dense layer moved by inertia, gradually expanding and transferring part of the energy to the environment.

Here, $\omega_t$ is the increment of hydrodynamic instability development derived in [22], $L_\rho = 1/\frac{\partial \ln \rho}{\partial z}$ is the density gradient scale, and $l_p(xl)$ is the turbulent pulsation size and depends on the width of the turbulence zone *xl*.

The authors of [21] suggest that

$$l_p = \alpha L_{mix}, \quad (16)$$

where $L_{mix}$ is the current size of the turbulent zone ($L_{mix} \approx xl$ in the experiment in Fig. 3a), while the value of α should be given *a priori*.

A program has been written that allows equation (14), (15) to be solved making allowance for (16).

The averaged values of layer acceleration $g = -\frac{1}{\rho} \cdot \frac{\partial P}{\partial z}$ and $L_\rho$ are taken from the numerical calculation results using the *Atlant_C* software.

It should be noted that the estimate $L_{mix} \approx \approx \alpha^4 \ln(\rho_1/\rho_2) g t^2$ is made in [21] for the case of contact between two incompressible media ($\rho_1$ and $\rho_2$) in the field of constant acceleration *g* (the acceleration is directed from the less dense medium toward the more dense one).

There are two stages of film acceleration: (1) when exposed to a laser pulse, the layer is accelerated due to reactive and thermal pressure from the vaporized plasma side, $g = +(3–4) \cdot 10^{12}$ cm/c$^2$ on the front side; (2) the layer is decelerated in the atmosphere, $g = -(1–2) \cdot 10^{11}$ cm/c$^2$ on the back side of the layer. The data are taken from numerical calculations in the *Atlant_C* software.

In numerical calculations, the value of α (*alfa*) is varied so that by the time the dense layer is flying past the slit, its width Δ*L* (*delta_L*) is equal to the value measured in the experiment [20].

The "broadening" due to turbulent mixing of the layers accelerated by the laser pulse in the case of the first and second types of film irradiation is shown in Fig. 4. The time moment *t* = 1150 ns when the layer is "seen" through the slit is given.

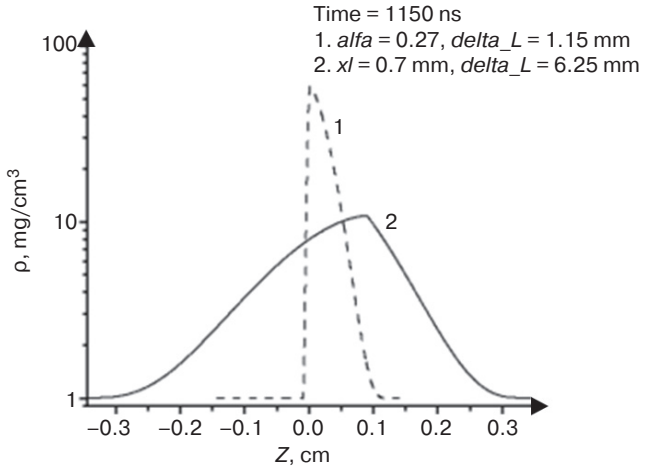


**Fig. 4.** Density of the accelerated layers obtained in calculations: 1—film is irradiated by a laser flux without flux perturbation, 2—introducing flux perturbation by dint of the grid, *xl* is a grid cell size, $l_p = xl$ [20]

## MODELING EXPERIMENTS ON IRRADIATION OF TWO-LAYER TARGETS AND FORMATION OF FINE STRUCTURES

In the third series of experiments, two-layer targets are irradiated in the form of a 100 μm aluminum layer followed by a ~5 mm plexiglass layer. The laser beam is incident on the aluminum side. The focus spot radius on the target surface is 50–70 μm. In the plexiglass, extended craters about 1 mm long are observed, while one or two narrow channels over 100–600 μm long are formed near its top (Fig. 5) [16, 23].

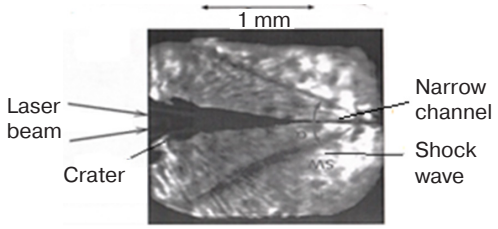


**Fig. 5.** Two-layer target after laser irradiation. The incident laser beam is shown on the left [23]

Calculations of the interacting laser pulses with targets are performed using the *NUTCY* software. In the calculated area, laser beams propagate strictly along the *OZ* axis, while refraction and self-focusing of light beams are not considered. The problem statement for modeling experiments is shown in Fig. 6.

The following parameters are used: focus spot radius $R_f = 50$ μm at Gaussian intensity distribution in the spot; the absorbed laser pulse energy 40 J; aluminum foil 100 μm thick and having initial density 2.7 g/cm$^3$ with plexiglass having initial density 1.19 g/cm$^3$ behind it; calculation area is a cylinder having radius $R_0 = 0.5$ mm and length *OZ* = 1.5 cm.

The two-dimensional distributions of density and temperature of the matter obtained in calculations in the *NUTCY* software are shown in Fig. 7. The length scale (*R* and *Z*) is given in units of $10^{-2}$ cm. The temperature scale is given in units of 100 eV. The corresponding density and temperature intervals are shown in the tables on the right and are represented as tonality in the figure (white–gray–black).

The plasma density and temperature distribution along the *OZ* axis as well as the density distribution along the radius at $Z_0 = 1$ cm (the initial position of the condensed matter–plasma boundary) is shown in Fig. 8.

Calculations in the *NUTCY* software allow modeling processes of forming the flaring plasma and extended crater in the condensed target. However, additional considerations and the development of a physical and mathematical model are required to explain the appearance of narrow channels in plexiglass.

The primary reason for the formation of narrow channels in plexiglass is the development of self-focusing of the laser beam in the plasma due to the

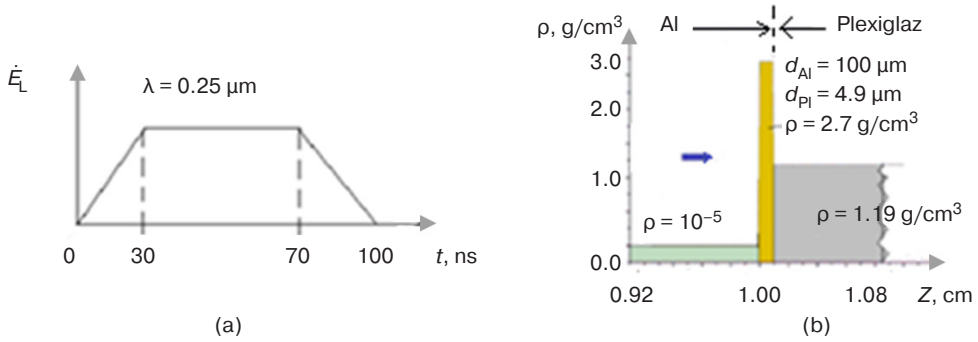


**Fig. 6.** Problem statement: temporal shape of the laser pulse (a); target parameters (b) [23]

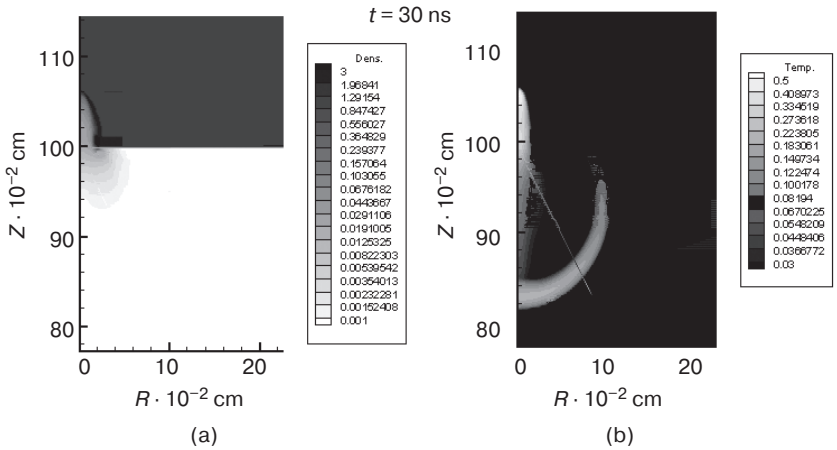


**Fig. 7.** Density ρ($R$, $Z$), g/cm$^3$ (a) and temperature $T$($R$, $Z$), $10^2$ eV (b) fields calculated for time moment $t$ = 30 ns [23]

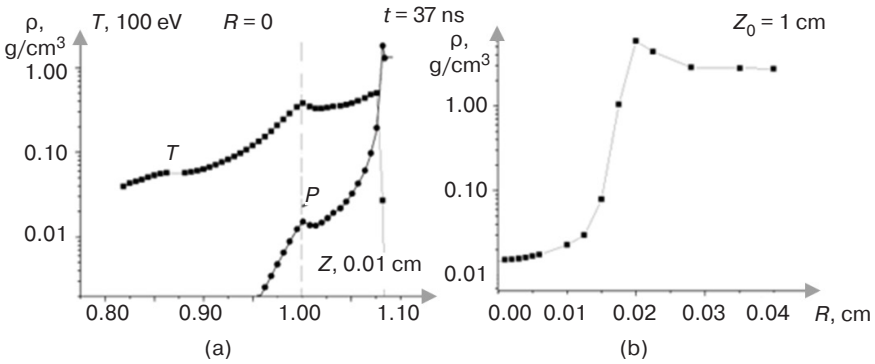


**Fig. 8.** Distribution of density ρ and temperature $T$ in the plasma along the axis $OO_1$ ($R$ = 0) at time moment $t$ = 37 ns (a); dependence of density ρ on radius $R$ at this moment at $Z_0$ = 1 cm (b) [23]

thermal mechanism. In the presence of the extended plasma, due to small perturbations of the laser beam intensity near the axis, the region of high temperature arises, thus resulting in "squeezing" of the plasma in the transverse direction. Due to refraction, beams gather toward the axis, in turn resulting in further formation of the low-density channel in the plasma. In case of small perturbations, an estimate of the threshold intensity $I_{th}$ for the thermal mechanism (in units of $10^{14}$ W/cm$^2$) is given in [24], as follows:

$$I_{th} \geq 2 \cdot 10^5 (\rho_{cr}/\rho)^3 \frac{T^5 \lambda^2}{Z_i^2 L_{pl}^2}. \qquad (17)$$

Here, temperature $T$ is given in keV units (~11.6 mln degrees), the plasma longitudinal channel scale $L_{pl}$ and emission wavelength λ are given in μm, while $Z_i$ is the average ion charge. The typical plasma parameters for conditions of the discussed experiments are the following: $Z_i$ = 4–6, $L_{pl}$ = 1000 μm, $T$ = 0.1 keV and λ = 0.25 μm, whence $I_{th} \geq 2 \cdot 10^{10}$ W/cm$^2$.

It is also possible to use a strictional (ponderomotive) mechanism of self-focusing, where the channel of reduced density is formed due to the action of ponderomotive force in the plasma in which beams are focused. However, the intensity perturbation threshold in this case is two orders of magnitude greater than in the case of thermal self-focusing.

In order to more accurately account for the above-mentioned effects in nonuniform plasma, it is necessary to use mathematical modeling methods involving the development of new programs to calculate the plasma dynamics equations together with nonlinear Maxwell equations[7].

The results of numerical modeling of laser beam self-focusing according to the simplified model of laser beam evolution in the conducting medium are given in [26]. This model implies the Gaussian distribution of radiation intensity in cylindrical beam $E^2(r,z) = E_0^2 \cdot \exp\left(-\frac{r^2}{a^2(z)}\right)$, where $E$ is electric intensity in the laser beam, $a(z)$ is effective radius changing as the radiation propagates along the $OZ$ axis.

Assuming that the permittivity depends on the law (paraxial approximation):

$$\varepsilon(z,r) = \varepsilon_0(z) + \beta(z)\cdot r^2, \quad \beta = \left.\frac{\partial\varepsilon}{\partial(r^2)}\right|_{r=0} \qquad (18)$$

the following equation for describing the dimensionless beam radius $f = \frac{a(z)}{a_0}$ may be written as (see more details in [27, 28]):

$$\varepsilon_0 \frac{df}{dz^2} + \frac{1}{2}\frac{d\varepsilon_0}{dz}\frac{df}{dz} = \frac{c^2}{\omega^2 a_0^4 f^3} - \beta(z) f. \qquad (19)$$

The first term on the right in equation (19) describes beam diffraction, while the second term describes self-focusing.

In case of strictional (or ponderomotive) mechanism:

$$\beta(z) = \left(\frac{\omega_p}{\omega}\right)^2 \frac{\alpha I_0}{f^2 a_0^2} e^{-\alpha I_0}, \quad \alpha = \frac{e^2}{8 m_e \cdot \omega^2 T_e}, \quad I_0 = E_0^2 \sqrt{\frac{\varepsilon_0(0)}{\varepsilon_0(z)}}. \qquad (20)$$

In case of a thermal mechanism:

$$\beta(z) = \left(\frac{\omega_p}{\omega}\right)^2 \cdot \frac{\sigma E_0^2}{8\chi_0 T_e^{3.5}} \cdot \sqrt{\frac{\varepsilon_0(0)}{\varepsilon_0(z)}} \cdot \frac{1}{f^2} = \frac{9}{16} \cdot \frac{\nu_{ei}^2}{\omega^2 T_e^2} \cdot I_0, \qquad (21)$$

where $\sigma$ is high-frequency electrical conductivity; $\nu_{ei}$ is the effective frequency of electron-ion collisions.

Equations (18)–(21) are solved numerically on the given density profiles $\rho(z)$ and the fixed value of electronic temperature $T(z)$.

The laser radiation and plasma parameters are taken from [23]: $I = 5 \cdot 10^{12}$ W/cm$^2$, $\rho_{cr} = 0.1354$ g/cm$^3$, $T(z) = 0.1$ keV, ion charge $Z_i = 6$, and plasma length $0 \le z \le 0.1$ cm. The exponential density profile is given: $\rho = \rho_{cr} \cdot \exp(-B(0.1 - z))$, $B = 40$ cm$^{-1}$.

The evolution of the dimensionless radius of beam $f_{th}$ along the $OZ$ axis for initial beam $a_0 = 35$ (1) and 100 μm (2) is shown in Fig. 9a. In both cases, self-focusing of light beams is observed due to the thermal mechanism. The strictional mechanism does not appear ($f_{str} > 1$).

The beam having initial radius 100 μm has decreased to dimensions $f < 10^{-3}$. The calculation is discontinued. The beam with initial radius 35 μm begins to increase in cross section after reaching the minimum value of $f = 2 \cdot 10^{-3}$. The first focus occurs at plasma density $\rho = 0.00243$ g/cm$^3$, i.e., $\rho/\rho_{cr} \approx 0.2$.

The development of thermal self-focusing of the laser beam in the crater plasma formed during irradiation of the condensed target by the high-power laser results in increasing intensity by 2–3 orders of magnitude. Further, the strictional mechanism near the critical surface may already dominate.

The beam evolution in the case of the ponderomotive (strictional) self-focusing development is shown in Fig. 9b. The initial beam radius $a_0$ = = 10 μm, $I = 5 \cdot 10^{16}$ W/cm$^2$. In this calculation series, $\rho_{cr} = 0.0677$ g/cm$^3$; $T(z) = 1$ keV; and ion charge $Z_i = 12$. In this case, it can be seen that the self-focusing increases much faster due to the strictional mechanism (red line) than due to the thermal mechanism (blue line).

When condition $I \cdot \lambda^2 > 10^{14}$ (W/cm$^2$)·μm$^2$ is fulfilled, "hot spots" arise near the critical surface where fluxes of above-thermal electrons are formed [2, 3]. These electrons penetrate deep into the cold condensed matter whose trace is observed in the discussed experiments near the crater top (Fig. 5).

The physico-mathematical models and numerical programs described above, which have been tested in experiments carried out using the powerful KrF-laser facility at GARPUN, reproduce the experimental data at a good level of accuracy with different types of targets and under various conditions of natural experiments. These circumstances allow the predictive mathematical modeling results of planned large-scale experiments (at the level of absorbed laser energy ~1 MJ) to be treated with confidence.

[7] The numerical modeling results of thermal self-focusing of the laser beam in plasma at the 3rd harmonic of Nd-laser ($\lambda$ = 0.35 μm) are given in [25] where the geometric optics model is used for describing the propagation of laser beams in a weakly heterogeneous medium ($\lambda << L_\rho$), but without paraxial approximation and hypothesis of the beam quasi-stationarity.

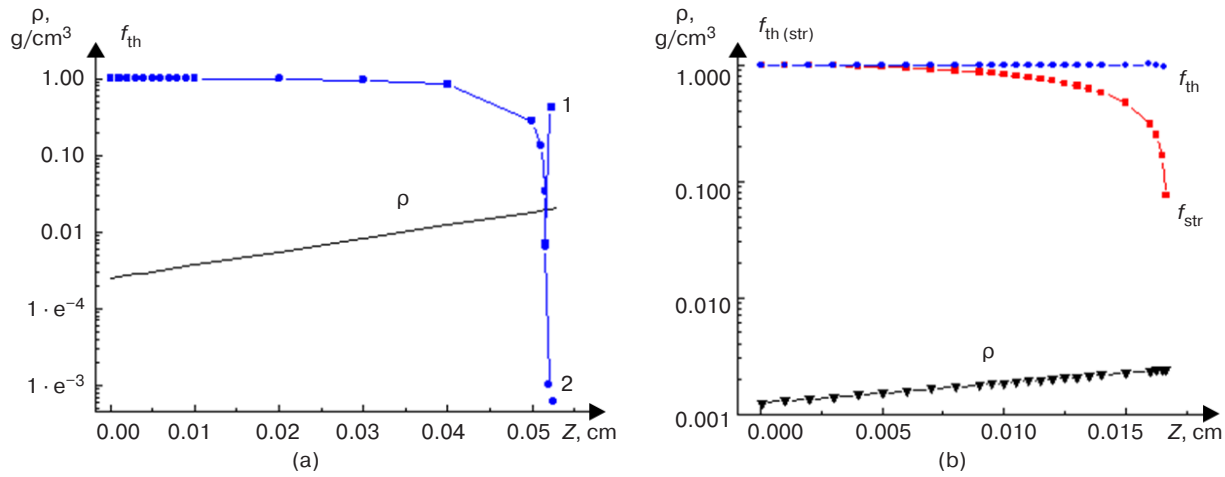


**Fig. 9.** Changing dimensionless beam radius on exponential plasma density profile: blue lines denote thermal mechanism; red line denotes strictional mechanism; and black line denotes density profile. (a) $I = 5 \cdot 10^{12}$ W/cm$^2$, (b) $I = 5 \cdot 10^{16}$ W/cm$^2$ [26]

## ON POSSIBLE TARGET DESIGN IN THE FORM OF A DOUBLE-SIDED CONE FOR AN EXCIMER DRIVER

It is conditionally possible to distinguish four main directions of promising applications of thermonuclear microbursts initiated by laser pulses. These are: (1) modeling substance behavior in laboratory conditions at very high energy concentrations and consequences of nuclear explosions, testing of corresponding numerical programs, as well as other applied tasks; (2) nuclear power engineering and development of new reactor types; (3) modeling astrophysical phenomena; and (4) development of rocket engines for interplanetary flights [2]. Generally speaking, the driver requirements for each of these directions can differ significantly. In the present paper, only the second direction is discussed.

It was stated in the introduction that, to date, no final choice has been made regarding the type of driver for the laser fusion reactor. At the first stage, the reactor function according to a hybrid scheme when the main energy is apparently obtained through the fission of heavy element nuclei (uranium), with this process being controlled by neutron fluxes from thermonuclear microbursts initiated by laser flares [29, 30]. This type of reactor is safer than those based on nuclear fission reactions only, since its "assemblies" are subcritical; moreover, the frequency of laser shots can decrease as fissile elements accumulate in blankets. The fuel of such reactors does not require pre-enrichment of uranium, since its power cycle can start with natural uranium $U^{238}$. Since the driver itself can be placed in an adjacent building at the distance of about 10 m from the reactor, the fission chain reactions can be quickly silenced by turning off the laser. It is possible to organize the fissile element production regime in such a way that the retrieval of the reactions would be an extremely rare procedure carried out directly on the plant premises or in another specially equipped location. In this way, the probability of terrorist takeover of these resources would be minimized, and the rooms where the radioactive elements are stored would be reliably protected from potential bomb blasts.

Nuclear reactions produce unique elementary particles including neutrinos and positrons. External magnetic fields allow the selection of charged particles and their temporary storage [2].

As mentioned above, the solid-state Nd-laser is planned to achieve high gain factors in a single thermonuclear microburst ($G >> 1$ is "ignition"). To achieve large values of $G$, it is necessary to compress the fuel to densities 1000 times greater than the density of the liquid DT mixture in order to initiate the fusion combustion wave. Due to development of hydrodynamic instability and mixing [2], such conditions have not yet been achieved in inertial thermonuclear fusion targets. On the other hand, achieving $G \sim 1$ is an independent goal of practical importance. Indeed, Fig. 10 shows a schematic of the nuclear-thermonuclear power plant with laser excitation of fusion microbursts [30]. Here, $\eta$ is the laser efficiency; $\beta$ is the conversion efficiency of thermal energy into electrical energy; $\phi$ is the fraction of energy providing reactor operation; $f$ is the frequency of laser shots; $E_L$ is the energy in the laser pulse; $W_t = fKE_L$ is the thermal power generated in the reactor; $W_n$ is the power, which a consumer gets (netto-power); $K = (0.2 + 0.8M)G$ is the reactor energy gain factor; $M$ is the energy multiplication factor in the reactor uranium blanket; $(1/\eta - 1)fE_L$ is the laser pumping energy loss. In order to "close" the energy cycle, the following inequality should be fulfilled:

$$(1 - \phi)\beta(0.2 + 0.8M)G > 1/\eta. \qquad (22)$$

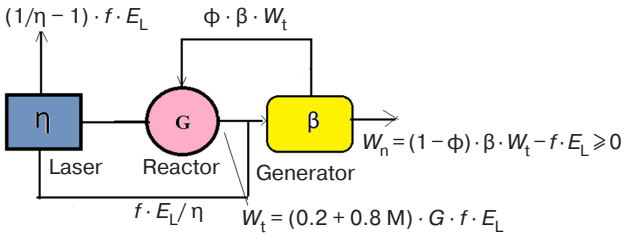


**Fig. 10.** Structural diagram of the hybrid nuclear-thermonuclear station [32, 33]

It follows from (22) that the gain factor should be $G \geq 1$ at $\phi = 0.2$, $\beta = 0.4$, $\eta = 0.05$, and $M = 60$. The use of a conical target and KrF-laser as the hybrid reactor driver is proposed in [31]. The laser pulse would consist of two long parts (accelerating) pulse with $\tau_1 \approx 100$ ns and a series of short pulses with $\tau_2 \approx 0.01$–$0.1$ ns. Due to the deformation of cone walls by strong SWs formed near its apex, it is virtually impossible to achieve compression of the fuel to densities significantly exceeding the normal wall density (i.e., 10–20 g/cm$^3$) in such a target design; however, this is not required for achieving gain factors $G \sim 1$. Short laser pulses injected through special holes near the cone apex would carry out local retention and additional heating of the compressed fuel.

The schematic of the two-sided conical target and its irradiation with laser beams taken from [32, 33] is shown in Fig. 11. The upper part of Fig. 11a shows an axial section of the target. The trigger (outer radius $R_0$) consists of polymer material *2* and a low-density substance (foam, aerogel) *3* required for "smoothing out" ablative pressure disturbances at the initial stage of the trigger acceleration. The low-density layer reduces the impact of small-scale disturbances of the laser flux, which can develop in the extended plasma due to self-focusing and forced Brillouin–Mandelstam scattering (BLS) and affect the stability of the flight. Next is a thin layer of gold *4*, followed by vacuum *5* and *6* comprising a layer of condensed DT fuel. The thin gold layer in the trigger increases the fuel compression ratio (in one-dimensional calculations). Using cryogenic DT fuel also allows the compression ratio to be increased[8].

The general scheme of the target in the form of counter cones is shown in Fig. 11b, while its central part is shown separately in Fig. 11c. The layer of low-density substance (foam in Fig. 11c) for "smoothing out" perturbations of ablative pressure of short pulses is located at the cone apex between the thin inner gold layer and the target outer chamber.

To achieve the level $G \sim 1$, it is sufficient to compress the condensed fuel by 30–50 times compared to the density of the liquid DT mixture. The entire compression process occurs mainly on the incident and reflected SW; under these conditions, it may be expected that mixing would not result in a catastrophic situation (i.e., in a decrease in the neutron yield by orders of magnitude compared to the results of one-dimensional calculations).

The calculation results performed in the spherical version of the *Atlant_Sp* software are given in [32], while those carried out in *SND* program developed at RFNC–VNIIEF [34, 35] are given in [33]. It should be noted that the comparative calculations carried out earlier using the *Atlant_Sp* and *SND* programs show close results at the same formulation of physical problems [36].

Numerical calculations show that thermonuclear yield $G \sim 1$ can be achieved in such a target design using pulses in the "long + short" mode at the level of absorbed laser energy ~1 MJ.

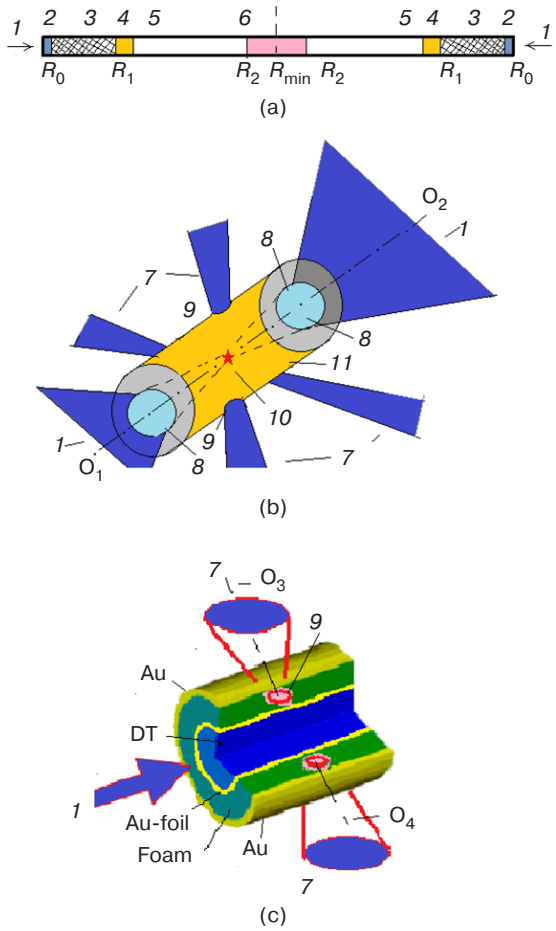


**Fig. 11.** Scheme of the two-sided conical target (a) and its irradiation by long + short laser pulses, $O_1O_2$ is the symmetry axis (b); (c) central part of the conical target. *1* is laser beams (long pulses) accelerating the trigger, *2* is the trigger dense layer, *3* is the foam layer, *4* is the thin gold layer, *5* is the vacuum gap, *6* is the cryogenic DT fuel layer, *7* is short laser pulses, *8* is the shell–trigger, *9* is holes for short pulses, *10* is the thermonuclear microburst, *11* is the gold target chamber with conical channels along the $O_1O_2$ axis, and $O_3O_4$ is the axis passing through target center in the plane perpendicular to symmetry axis $O_1O_2$ [32, 33]

[8] The impact of the development of self-focusing and hydrodynamic instabilities is not considered directly in calculations.

The calculations assume that cone walls are absolutely elastic and heat-resistant. The formation of the "shell–wall" boundary layer is not considered there. The problem has perfect symmetry with respect to the top of the truncated cone (the $O_3O_4$ axis through which the symmetry plane perpendicular to the $O_1O_2$ axis passes is shown in Fig. 11c). The process of compression and initiation of thermonuclear reactions in such targets may be conventionally divided into two stages. At the first stage, a long laser pulse accelerates the trigger that moves to the top of the cone and compresses the DT fuel. When the SW reaches the apex of the truncated cone and is reflected there, a series of short pulses (total duration about ~0.1 ns, total energy ~10% of the main heating pulse) is injected through the holes into the target in the plane perpendicular to the $O_1O_2$ axis. The purpose of these pulses is to ensure the dynamic retention of the compressed fuel and its additional heating (second stage).

The following two series of calculations of the target compression by a long pulse of KrF-laser of various time shapes are performed: (1) in the form of a triangle with time moments at tops $t_1 = 0$, $t_2 = 100$ ns, and $t_3 = 101$ ns; (2) in the form of a curved trapezoid with the tightened front smoothly rising ($t_2 - t_1 = 12$ ns) and with a subsequent rectangular pulse ($t_3 - t_2 = 10$ ns). The targets have the form of truncated cones with aspect ratios $R_0/R_{min} = 10–20$ (Fig. 11a). The gain factor $G > 1$.

Thus, using UV laser pulses with energies of ≈2 MJ and targets in the form of counter truncated cones allows providing the "thermonuclear flare"[9].

## DISCUSSION OF RESULTS AND CONCLUSIONS

The main elements of the scheme discussed in the paper are individually tested in small-scale natural and numerical experiments.

Experiments with conical laser targets performed at the Prokhorov General Physics Institute of the RAS on a solid-state infrared laser are described in the review [37].

The amplification of picosecond pulses generated by the Ti:sapphire laser together with long UV pulse is tested at the GARPUN-MTV facility (FIAN, Russia) [38, 39].

The impact of hydrodynamic instability and interaction with the wall during laser acceleration of the trigger in the conical channel remain insufficiently studied; this is also the case with the development of self-focusing and BLS in the extended plasma. Semiempirical physico-mathematical models and software packages are developed based on numerical calculations and natural experiments carried out on various laboratory benches [40–44]. Direct mathematical modeling of these phenomena requires the use of high-performance supercomputers and parallel computing algorithms. Such work is being carried out, in particular, at the MIREA – Russian Technological University [45].

In the USA, the *ELECTRA* program for constructing a powerful KrF-laser-based LTF research facility operating in frequency mode has been announced [46–51].

The physico-mathematical models and programs, which adequately describe the model data from experiments performed at the GARPUN laser facility, provide a basis for target designs for future large-scale reactor-scale experiments.

Figure 12 shows the proposed scenario for the development of laser fusion research as applied to the creation of a power plant: the first stage is research and development (R&D), while the second stage is the experimental and technological development (ETD), the third stage is the development of a pilot and experimental reactor (DPER), and the fourth stage is the development of a commercial reactor (DCR). The abscissa axis shows the estimated costs of overcoming these stages.

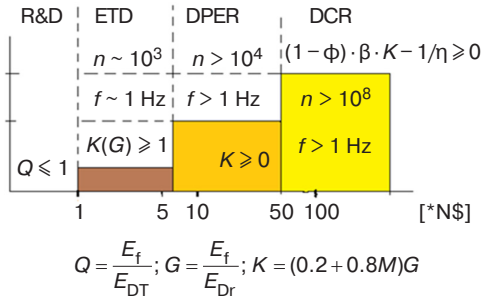


**Fig. 12.** Assumed scenario for the development of inertial fusion research (drawn by the Author). *n*—resource, *f*—frequency of microbursts, *N$—capital expenditure, $N = 1$—expenditure of R&D stage (footstep), $E_{Dr}$—driver energy, and $E_L$—laser pulse energy. $E_{Dr} = E_L$

There are several criteria for characterizing fusion efficiency:

1) $Q = E_f/E_{DT} = 1$ is the "physical threshold of fusion reactions," when the released fusion energy $E_f$ equals the energy invested in the DT plasma from the third-party source $E_T$;
2) $G = E_f/E_{Dr}$, "gain" is gain or "flash criterion." As a rule, this coefficient is an order of magnitude smaller than $Q$ at the same $E_f$, since a significant part of the energy is "lost" with the vaporized inert material of the target and does not get into the compressed fuel;
3) $K = (0.2 + 0.8M)\cdot G$ is the reactor gain factor allowing also for the energy gain $M$ due to fission reactions;

[9] We shall mean $G = 2–3$ by "flash."

4) $C_E = (1 - \phi)\beta K - 1/\eta$ is the "plant energy efficiency" parameter.

At the R&D stage, the main challenge is the physical threshold of thermonuclear reactions. American scientists have managed to achieve this[10] [7] to approach the value $G \sim 1$ at the NIF facility. On this basis, it can be said that they are ready to move to the second stage, i.e., ETD.

Overcoming this stage requires a repetition frequency of laser pulses at the level of $f \sim 1$ Hz and the consequent feeding of targets into the focus of laser beams at the same frequency, as well as providing "resource $n$," i.e., uninterrupted operation of the entire system at least for an hour ($n \sim 10^3$).

At the ETD stage, it is necessary to provide $K(G) \geq 1$, i.e., to check the possibility of the blanket functioning in the frequency mode of loads, as well as "some resource" $n \sim 10^3$, i.e., ensuring the functioning of the whole reactor for a certain period of time without stopping or interrupting operations.

At the DPER stage, it is necessary to reach the level of "closing" the reactor power cycle ($C_E > 0$) and ensuring resource $n > 10^4$, i.e., the uninterrupted operation of such an experimental reactor for several hours (possibly even days).

The final stage is the development of a commercial reactor. Such a reactor could operate non-stop for several decades and would be economically viable compared to other sources of energy.

[10] Kritcher A. and HIBRYD-E ICF team. Initial results from HYBRID-E DT experiment N210808 with >1.3 MJ yield. *IFSA Virtual Meeting*. September 2021. LLNL-PRES-826367. P. 16. https://www.aps.org/units/maspg/meetings/upload/obenschain-11172021.pdf. Accessed February 07, 2023.

## ACKNOWLEDGMENTS

The study was performed within the National Center for Physics and Mathematics, Gas Dynamics and Explosion Physics Program on the topic "Investigation of Physical Processes during Controlled Thermonuclear Fusion and in Stellar Systems."

## REFERENCES

1. Basov N.G., Krokhin O.N. Conditions for heating up of a plasma by the radiation from an optical generator. *Sov. Phys. JETP.* 1964;19(1):123–126. Available from URL: http://www.jetp.ras.ru/cgi-bin/dn/e_019_01_0123.pdf
2. Basov N.G., Lebo I.G., Rozanov V.B. *Fizika lazernogo termoyadernogo sinteza* (*Physics of Laser Thermonuclear Fusion*). Moscow: Znanie; 1988. 172 p. (in Russ.).
3. Atzeni S. Laser driven inertial fusion: The physical basis of current and recently proposed ignition experiments. *Plasma Phys. Control Fusion*. 2009;51(12):124029. https://doi.org/10.1088/0741-3335/51/12/124029
4. Garanin S.G., Bel'kov S.A., Bondarenko C.V. The concept of building a laser installation UFL-2M. In: *Doklady 39 Mezhdunarodnoi* (*Zvenigorodskoi*) *konferentsii po fizike plazmy i upravlyaemomu termoyadernomu sintezu* (*Proc. 39th Intern.* (*Zvenigorod*) *Conf. on Plasma Physics and Control. Thermonuclear Fusion*). Zvenigorod; 2012. P. 17 (in Russ.).
5. Moses E.I. and NIC Collaboration. The National Ignition Campaign: status and progress. *Nucl. Fusion.* 2013;53(10):104020. https://doi.org/10.1088/0029-5515/53/10/104020

## СПИСОК ЛИТЕРАТУРЫ

1. Басов Н.Г., Крохин О.Н. Условия разогрева плазмы излучением оптического генератора. *ЖЭТФ.* 1964;46(1):171–175.
2. Басов Н.Г., Лебо И.Г., Розанов В.Б. *Физика лазерного термоядерного синтеза*. М.: Знание; 1988. 176 с.
3. Atzeni S. Laser driven inertial fusion: The physical basis of current and recently proposed ignition experiments. *Plasma Phys. Control Fusion*. 2009;51(12):124029. https://doi.org/10.1088/0741-3335/51/12/124029
4. Гаранин С.Г., Бельков С.В., Бондаренко С.В. Концепция построения лазерной установки УФЛ-2М. В сб.: *Доклады XXXIX Международной* (*Звенигородской*) *конференции по физике плазмы и управляемому термоядерному синтезу.* Звенигород; 2012. С. 17.
5. Moses E.I. and NIC Collaboration. The National Ignition Campaign: status and progress. *Nucl. Fusion.* 2013;53(10):104020. https://doi.org/10.1088/0029-5515/53/10/104020
6. Ebrardt J., Chapt J.M. LMJ on its way to fusion. *J. Phys: Conf. Ser:* 2010;244(3):032017. https://doi.org/10.1088/1742-6596/244/3/032017

6. Ebrardt J., Chapt J.M. LMJ on its way to fusion. *J. Phys: Conf. Ser:* 2010;244(3):032017. https://doi.org/10.1088/1742-6596/244/3/032017
7. Le P.S., Hopkins B.L.F., Divol L., et. al. Fusion energy output greater than the kinetic energy of an imploding shell at the National Ignition Facility. *Phys. Rev. Lett.* 2018;120(24):245003. https://doi.org/10.1103/PhysRevLett.120.245003
8. Clery D. Laser-powered fusion effort near 'ignition'. *Science.* 2021;373(6557):841. https://doi.org/10.1126/science.373.6557.841
9. Clark D.S., Casey D.T., Weber C.R., et al. Exploring implosion designs for increased compression on the National Ignition Facility using high density carbon ablation. *Phys. Plasmas*. 2022;29(5):052710. https://doi.org/10.1063/5.0087052
10. He X.T., Zhang W.Y., and Chinese ICF Team. Advances in the national inertial fusion program in China. *EPJ Web of Conference*. 2013;59:001009. https://doi.org/10.1051/epjconf/20135901009
11. Zhen W., Wei X., Zhu Q., Jing F., et al. Laser performance of the SG-III laser facility. *High Power Laser. Sci. Eng*. 2016;4:e21. https://doi.org/10.1017/hpl.2016.20
12. Lebo I.G., Tishkin V.F. *Issledovanie gidrodinamicheskoi neustoichivosti v zadachakh lazernogo termoyadernogo sinteza* (*Investigation of Hydrodynamic Instability in Problems of Laser Thermonuclear Synthesis*). Moscow: Fizmatlit; 2006. 304 p. (in Russ.). ISBN 5-9221-0683-X
13. Kuzenov V.V., Lebo A.I., Lebo I.G., Ryzhkov S.V. *Fiziko-matematicheskie modeli i metody rascheta vozdeistviya moshchnykh lazernykh i plazmennykh impul'sov na kondensirovannye i gazovye sredy* (*Physical-Mathematical Models and Numerical Methods of Simulation of High Power laser and Plasma Pulses Interaction with Condense and Gas Medias)*. Moscow: BMSTU; 2015. 327 p. (in Russ.). ISBN 978-5-7038-4183-9
14. Samarskii A.A. *Teoriya raznostnykh skhem* (*Difference Scheme Theory*). Moscow: Nauka; 1990. 616 p. (in Russ.). ISBN 5-02-014576-9
15. Samarskii A.A., Popov Yu.P. *Raznostnye metody resheniya zadach gazovoi dinamiki* (*Difference methods for solving problems of gas dynamics*). Moscow: Nauka; 1992. 422 p. (in Russ.). ISBN 5-02-014577-7
16. Zvorykin V.D., Lebo I.G. Laser and target experiments on KrF GARPUN laser installation at FIAN. *Laser Part. Beams*. 1999;17(1):69–88. https://doi.org/10.1017/S0263034699171064
17. Richmyer R.D. Taylor instability in shock acceleration of compressible fluids. *Commun. Pure Appl. Math.* 1960;13(2):297–319. https://doi.org/10.1002/cpa.3160130207
18. Meshkov E.E. The instability of two gases surface, which accelerated by shock wave. *Izvestiya AN SSSR. Ser. Mekhanika Zhidkosti i Gaza*. 1969;5:151–158 (in Russ.). Available from URL: https://mzg.ipmnet.ru/ru/get/1969/5/151-158
19. Zvorykin V.D., Lebo I.G. Application of a high power KrF laser for the study of supersonic gas flows and the development of hydrodynamic instability in layered media. *Quantum Electron.* 2000;30(6):540–544. https://doi.org/10.1070/QE2000v030n06ABEH001761
7. Le P.S., Hopkins B.L.F., Divol L., et. al. Fusion energy output greater than the kinetic energy of an imploding shell at the National Ignition Facility. *Phys. Rev. Lett.* 2018;120(24):245003. https://doi.org/10.1103/PhysRevLett.120.245003
8. Clery D. Laser-powered fusion effort near 'ignition'. *Science.* 2021;373(6557):841. https://doi.org/10.1126/science.373.6557.841
9. Clark D.S., Casey D.T., Weber C.R., et al. Exploring implosion designs for increased compression on the National Ignition Facility using high density carbon ablation. *Phys. Plasmas*. 2022;29(5):052710. https://doi.org/10.1063/5.0087052
10. He X.T., Zhang W.Y., and Chinese ICF Team. Advances in the national inertial fusion program in China. *EPJ Web of Conference*. 2013;59:001009. https://doi.org/10.1051/epjconf/20135901009
11. Zhen W., Wei X., Zhu Q., Jing F., et al. Laser performance of the SG-III laser facility. *High Power Laser. Sci. Eng*. 2016;4:e21. https://doi.org/10.1017/hpl.2016.20
12. Лебо И.Г., Тишкин В.Ф. *Исследование гидродинамической неустойчивости в задачах лазерного термоядерного синтеза*. М.: Физматлит; 2006. 304 с. ISBN 5-9221-0683-X
13. Кузенов В.В., Лебо А.И., Лебо И.Г., Рыжков С.В. *Физико-математические модели и методы расчета воздействия мощных лазерных и плазменных импульсов на конденсированные и газовые среды*. М.: Изд-во МГТУ им. Н.Э. Баумана; 2015. 327 с. ISBN 978-5-7038-4183-9
14. Самарский А.А. *Теория разностных схем*. М.: Наука; 1990. 616 с. ISBN 5-02-014576-9
15. Самарский А.А., Попов Ю.П. *Разностные методы решения задач газовой динамики.* М.: Наука; 1992. 422 с. ISBN 5-02-014577-7
16. Zvorykin V.D., Lebo I.G. Laser and target experiments on KrF GARPUN laser installation at FIAN. *Laser Part. Beams*. 1999;17(1):69–88. https://doi.org/10.1017/S0263034699171064
17. Richmyer R.D. Taylor instability in shock acceleration of compressible fluids. *Commun. Pure Appl. Math.* 1960;13(2):297–319. https://doi.org/10.1002/cpa.3160130207
18. Мешков Е.Е. Неустойчивость границы раздела двух газов, ускоряемой ударной волной. *Известия АН СССР. Сер. Механика жидкости и газа.* 1969;5:151–158. URL: https://mzg.ipmnet.ru/ru/get/1969/5/151-158
19. Зворыкин В.Д., Лебо И.Г. Применение мощного KrF-лазера для исследования сверхзвуковых течений газа и развития гидродинамических неустойчивостей в слоистых средах. *Квантовая электроника*. 2000;30(6):540–544.
20. Lebo I.G., Zvorykin V.D. The study of turbulent mixing zone development in laser shock tube experiments. *Phys. Scr*. 2008;2008(T132):014018. https://doi.org/10.1088/0031-8949/2008/T132/014018
21. Беленький С.З., Фрадкин Е.С. Теория турбулентного перемешивания. *Труды ФИАН.* 1965;29:207–233.
22. Фрадкин Е.С. Исследование устойчивости произвольного одномерного гидродинамического течения. *Труды ФИАН.* 1965;29:250–256.

[Original Russian Text: Zvorykin V.D., Lebo I.G. Application of a high power KrF laser for the study of supersonic gas flows and the development of hydrodynamic instability in layered media. *Kvantovaya Elektronika*. 2000;30(6):540–544 (in Russ.).]
20. Lebo I.G., Zvorykin V.D. The study of turbulent mixing zone development in laser shock tube experiments. *Phys. Scr*. 2008;2008(T132):014018. https://doi.org/10.1088/0031-8949/2008/T132/014018
21. Belen'kii S.Z., Fradkin E.S. Theory of turbulent mixing. *Trudy FIAN = Proceedings of the Lebedev Physics Institute*. 1965;29:207–233 (in Russ.).
22. Fradkin E.S. The investigation of the arbitrary 1D hydrodynamic flow stability. *Trudy FIAN = Proceedings of the Lebedev Physics Institute*.1965;29:250–256 (in Russ.).
23. Zvorykin V., Lebo I., Shutov A., Ustinovskii N. Self-focusing of UV radiation in 1 mm scale plasma in a deep ablative crater produced by 100 ns, 1 GW KrF laser pulse in the context of the ICF. *Matter Radiat. Extremes*. 2020;5(30):03540. https://doi.org/10.1063/1.5142361
24. Craxton R.S., Anderson K.S., Boehly T.R., et al. Direct drive inertial confinement fusion: A review. *Phys. Plasmas*. 2015;22(1):110501. https://doi.org/10.1063/1.4934714
25. Craxton R.S., McCrory R.L. Hydrodynamics of thermal self-focusing in laser plasmas. *J. Appl. Phys*. 1984;56(1):108. https://doi.org/10.1063/1.333742
26. Lebo I.G. About the modeling of light beam self-focusing in plasma at the irradiation of the target by power UV laser. *Russ. Technol. J*. 2021;9(1):79–86 (in Russ.). https://doi.org/10.32362/2500-316X-2021-9-1-79-86
27. Akhmanov S.A., Sukhorukov A.P., Khohlov R.V. Self-focusing and diffraction of light in nonlinear medium. *Sov. Phys. Usp.* 1968;10(3):609–636. https://doi.org/10.1070/PU1968v010n05ABEH005849
[Original Russian Text: Akhmanov S.A., Sukhorukov A.P., Khohlov R.V. Self-focusing and diffraction of light in nonlinear medium. *Uspekhi Fizicheskikh Nauk.* 1967;93(1):19–70 (in Russ.). https://doi.org/10.3367/UFNr.0093.196709c.0019]
28. Sodha M.S., Tripathi V.K. Nonlinear penetration of an inhomogeneous laser beam in an overdense plasma. *Phys. Rev. A.* 1977;16(5):2101–2104. https://doi.org/10.1103/PhysRevA.16.2101
29. Basov N.G., Subbotin V.I., Feoktistov L.P. Nuclear reactor with laser fusion neutron source. *Vestnik Rossiiskoi Akademii Nauk = Bulletin of the Russian Academy of Sciences.* 1993;63(10):787–884 (in Russ.).
30. Basov N.G., Belousov N.I., Grishunin P.A., et al. Hybrid reactor based on laser thermonuclear fusion. *Sov. J. Quantum Electronics*. 1987;17(10):1324–1332. https://doi.org/10.1070/QE1987v017n10ABEH010765
[Original Russian Text: Basov N.G., Belousov N.I., Grishunin P.A., Kalmykov Yu.K., Lebo I.G., Rozanov V.B., Sklizkov G.V., Subbotin V.I., Finkel'shtein K.I., Kharitonov V.V., Sherstnev K.B. Hybrid reactor based on laser thermonuclear fusion. *Kvantovaya Elektronika*. 1987;14(10):2068–2081 (in Russ.).]
31. Zvorykin V.D., Lebo I.G., Rozanov V.B. On the feasibility of the production of a source of the thermonuclear neutrons on the basis of a KrF laser. *Bulletin of the Lebedev Physical Institute*. 1997;9:15–22.
23. Zvorykin V., Lebo I., Shutov A., Ustinovskii N. Self-focusing of UV radiation in 1 mm scale plasma in a deep ablative crater produced by 100 ns, 1 GW KrF laser pulse in the context of the ICF. *Matter Radiat. Extremes*. 2020;5(30):03540. https://doi.org/10.1063/1.5142361
24. Craxton R.S., Anderson K.S., Boehly T.R., et al. Direct drive inertial confinement fusion: A review. *Phys. Plasmas*. 2015;22(1):110501. https://doi.org/10.1063/1.4934714
25. Craxton R.S., McCrory R.L. Hydrodynamics of thermal self-focusing in laser plasmas. *J. Appl. Phys*. 1984;56(1):108. https://doi.org/10.1063/1.333742
26. Лебо И.Г. О моделировании самофокусировки светового пучка в плазме при облучении мишеней мощным ультрафиолетовым лазером. *Russ. Technol. J*. 2021;9(1):79–86. https://doi.org/10.32362/2500-316X-2021-9-1-79-86
27. Ахманов С.А., Сухоруков А.П., Хохлов Р.В. Самофокусировка и дифракция света в нелинейной среде. *УФН*. 1967;93(1):19–70. https://doi.org/10.3367/UFNr.0093.196709c.0019
28. Sodha M.S., Tripathi V.K. Nonlinear penetration of an inhomogeneous laser beam in an overdense plasma. *Phys. Rev. A.* 1977;16(5):2101–2104. https://doi.org/10.1103/PhysRevA.16.2101
29. Басов Н.Г., Субботин В.И., Феоктистов Л.П. Ядерный реактор с лазерным термоядерным источником нейтронов. *Вестник Российской академии наук*. 1993;63(10):787–884.
30. Басов Н.Г., Белоусов Н.И., Гришунин П.А., Калмыков Ю.К., Лебо И.Г., Розанов В.Б., Склизков Г.В., Субботин В.И., Финкельштейн К.И., Харитонов В.В., Шерстнев К.Б. Гибридный реактор на основе лазерного термоядерного синтеза. *Квантовая электроника.* 1987;14(10):2068–2081.
31. Зворыкин В.Д., Лебо И.Г., Розанов В.Б. О возможности создания источника термоядерных нейтронов на основе KrF-лазера. *Краткие сообщения по физике*. 1997;(9–10):20–29.
32. Лебо И.Г., Исаев Е.А., Лебо А.И. Двухсторонняя лазерная коническая мишень для нейтронного источника ядерно-термоядерного реактора. *Квантовая электроника*. 2017;47(2):106–110.
33. Долголева Г.В., Лебо И.Г. К вопросу о разработке нейтронного источника для ядерно-термоядерного реактора с лазерным возбуждением. *Квантовая электроника*. 2019;49(8):796–800.
34. Долголева Г.В. Методы расчета движения двухтемпературного излучающего газа. *Вопросы атомной науки и техники. Сер. Методики и программы численного решения задач математической физики*. 1983;2(13):29–33.
35. Бельков С.А., Долголева Г.В. Модель среднего иона для расчета кинетики ионизации, населенностей возбужденных уровней и спектральных коэффициентов переноса излучения в программе СНДП. *Вопросы атомной науки и техники. Сер. Методики и программы численного решения задач математической физики.* 1992;1:59–61.
36. Долголева Г.В., Лебо А.И., Лебо И.Г. Моделирование сжатия термоядерных мишеней на уровне энергии лазера порядка 1 МДж. *Матем. моделирование*. 2016;28(1):23–32.

[Original Russian Text: Zvorykin V.D., Lebo I.G., Rozanov V.B. On the feasibility of the production of a source of the thermonuclear neutrons on the basis of a KrF laser. *Kratkie Soobshcheniya po Fizike*. 1997;(9–10):20–29 (in Russ.).]

32. Lebo I.G., Isaev E.A., Lebo A.I. Two-sided conical laser target for a neutron source of a hybrid nuclear-thermonuclear reactor. *Quantum Electronics*. 2017;47(2):106–110. https://doi.org/10.1070/QEL16277
[Original Russian Text: Lebo I.G., Isaev E.A., Lebo A.I. Two-sided conical laser target for a neutron source of a hybrid nuclear-thermonuclear reactor. *Kvantovaya Elektronika.* 2017;47(2):106–110 (in Russ.).]
33. Dolgoleva G.V., Lebo I.G. On the issue of neutron source development for a nuclear-thermonuclear reactor. *Quantum Electronics*. 2019;49(8):796–800. https://doi.org/10.1070/QEL16953
[Original Russian Text: Dolgoleva G.V., Lebo I.G. On the issue of neutron source development for a nuclear-thermonuclear reactor. *Kvantovaya Elektronika.* 2019;49(8):796–800 (in Russ.).]
34. Dolgoleva G.V. Methods of simulation of two temperature irradiated gas. *Voprosy Atomnoi Nauki i Tekhniki*. *Ser. Metodiki i Programmy Chislennogo Resheniya Zadach Matematicheskoi Fiziki*. 1983;2(13):29–33 (in Russ.).
35. Bel'kov S.A., Dolgoleva G.V. The model of average ion for the simulation of ionization kinetics, excited levels and spectral radiation transfer coefficients in SNDP program. *Voprosy Atomnoi Nauki i Tekhniki*. *Ser. Metodiki i Programmy Chislennogo Resheniya Zadach Matematicheskoi Fiziki*. 1992;1:59–61 (in Russ.).
36. Dolgoleva G.V., Lebo A.I., Lebo I.G. Simulation of a thermonuclear target drive at the 1 MJ laser energy level. *Math. Models Comput. Simul*. 2016;8(4):438–445. https://doi.org/10.1134/S2070048216040062
[Original Russian Text: Dolgoleva G.V., Lebo A.I., Lebo I.G. Simulation of a thermonuclear target drive at the 1 MJ laser energy level. *Matematicheskoe Modelirovanie*. 2016;28(1):23–32 (in Russ.).]
37. Krasyuk I.K., Semenov A.Yu., Charakhch'yan A.A. Use a conic targets in Inertial confinement fusion. *Quantum Electronics.* 2005;35(9):769–777. https://doi.org/10.1070/QE2005v035n09ABEH006128
[Original Russian Text: Krasyuk I.K., Semenov A.Yu., Charakhch'yan A.A. Use a conic targets in Inertial confinement fusion. *Kvantovaya Elektronika.* 2005;35(9):769–777 (in Russ.).]
38. Zvorykin V.D., Didenko N.V., Ionin A.A., et al. GARPUN-MTW: A hybrid Ti:Sapphire/KrF laser facility for simultaneous amplification of subpicosecond/nanosecond pulses relevant to fast-ignition ICF concept. *Laser Part. Beams*. 2007;25(3):435–451. https://doi.org/10.1017/S0263034607000559
39. Zvorykin V.D., Levchenko A.O., Ustinovskii N.N. Amplification of subpico second UV pulses in the multistage GARPUN-MTW Ti:sapphire–KrF-laser system. *Quantum Electronics*. 2010;40(5):381–385. https://doi.org/10.1070/QE2010v040n05ABEH014241
[Original Russian Text: Zvorykin V.D., Levchenko A.O., Ustinovskii N.N. Amplification of subpico second UV pulses in the multistage GARPUN-MTW Ti:sapphire–KrF-laser system. *Kvantovaya Elektronika.* 2010;40(5):381–385 (in Russ.).]
37. Красюк И.К., Семенов А.Ю., Чарахчьян А.А. Использование конических мишеней в исследованиях по инерциальному термоядерному синтезу. *Квантовая электроника.* 2005;35(9):769–777. URL: https://www.mathnet.ru/links/a64472a2c6918f95785286b47b113907/qe6128.pdf
38. Zvorykin V.D., Didenko N.V., Ionin A.A., et al. GARPUN-MTW: A hybrid Ti:Sapphire/KrF laser facility for simultaneous amplification of subpicosecond/nanosecond pulses relevant to fast-ignition ICF concept. *Laser Part. Beams*. 2007;25(3):435–451. https://doi.org/10.1017/S0263034607000559
39. Зворыкин В.Д., Левченко А.О., Устиновский Н.Н. Усиление субпикосекундных УФ импульсов в многокаскадной лазерной Ti:сапфир–KrF-системе ГАРПУН-МТВ. *Квантовая электроника.* 2010;40(5):381–385.
40. Неуважаев В.Е. *Математическое моделирование турбулентного перемешивания*. Снежинск: РФЯЦ-ВНИИТФ; 2007. 160 с. URL: https://math.csu.ru/new_files/students/lectures/ur_mat_fiz/neyvajaev_mat_model.pdf
41. Невмержицкий Н.В. *Гидродинамические неустойчивости и турбулентное перемешивание веществ. Лабораторное моделирование.* Саров: РФЯЦ-ВНИИЭФ; 2018. 245 с. ISBN 978-5-9515-0377-0
42. Янилкин Ю.В., Стаценко В.П., Козлов В.И. *Математическое моделирование турбулентного перемешивания в сжимаемых средах:* в 2-х т. Т. 1. Саров: РФЯЦ-ВНИИЭФ; 2019. 357 с. ISBN 978-5-9515-0421-0
43. Янилкин Ю.В., Стаценко В.П., Козлов В.И. *Математическое моделирование турбулентного перемешивания в сжимаемых средах:* в 2-х т. Т. 2. Саров: РФЯЦ-ВНИИЭФ; 2020. 407 с. ISBN 978-5-9515-0458-6
44. Разин А.Н. *Моделирование турбулентного перемешивания в газовых слойках*. Саров: РФЯЦ-ВНИИЭФ; 2020. 290 с. ISBN 978-5-9515-0434-0
45. Лебо И.Г., Обручев И.В. Моделирование двумерных вихревых течений в цилиндрическом канале с помощью параллельных вычислений на суперкомпьютере. *Russ. Technol. J*. 2022;10(1):60–67. https://doi.org/10.32362/2500-316X-2022-10-1-60-67
46. Obenschain S., Lehmlerg R., Kehne D., et al. High-energy krypton-fluoride laser for inertial fusion. *Appl. Opt.* 2015;54(31):F103–F122. http://dx.doi.org/10.1364/AO.54.00F103
47. Sethian J., Obenschain S. Fusion energy with krypton fluoride lasers and direct drive targets. *Fusion Sci. Technol*. 2012;61(1T):41–46. https://doi.org/10.13182/FST12-A13394
48. Wolford M.F., Sethian J.D., Myers M.C., Hegeler F., Giuliani J.L., Obenschain S.P. Krypton fluoride (KrF) laser for inertial fusion energy. *Fusion Sci. Technol*. 2013;64(2):179–186. https://doi.org/10.13182/FST12-502
49. Bodner S.E. The path to electrical energy using laser fusion. *High Power Laser Science and Engineering.* 2019;7:e63. https://doi.org/10.1017/hpl.2019.51
50. Schmitt A.J., Obenschain S.P. The importance of laser wavelength for driving inertial confinement fusion targets. I. Basic physics. *Phys. Plasmas*. 2023;30(1):012701. https://doi.org/10.1063/5.0118080
51. Schmitt A.J., Obenschain S.P. The importance of laser wavelength for driving inertial confinement fusion targets. II. Target design. *Phys. Plasmas*. 2023;30(1):012702. https://doi.org/10.1063/5.0118093

40. Neuvazhaev V.E. *Matematicheskoe modelirovanie turbulentnogo peremeshivaniya* (*The mathematical modeling of turbulent mixing*). Snezhinsk; 2007. 160 p. (in Russ.). Available from URL: https://math.csu.ru/new_files/students/lectures/ur_mat_fiz/neyvajaev_mat_model.pdf
41. Nevmerzhitskii N.V. *Gidrodinamicheskie neustoichivosti i turbulentnoe peremeshivanie veshchestv. Laboratornoe modelirovanie* (*Hydrodynamic instability and turbulent mixing of matters. The laboratory modeling*). Sarov; 2018. 245 p. (in Russ.). ISBN 978-5-9515-0377-0
42. Yanilkin Yu.V., Statsenko V.P., Kozlov V.I. *Matematicheskoe modelirovanie turbulentnogo peremeshivaniya v szhimaemykh sredakh* (*The mathematical modeling of turbulent mixing in compressed matters*): in 2 v. V. 1. Sarov; 2019. 357 p. (in Russ.). ISBN 978-5-9515-0421-0
43. Yanilkin Yu.V., Statsenko V.P., Kozlov V.I. *Matematicheskoe modelirovanie turbulentnogo peremeshivaniya v szhimaemykh sredakh* (*The mathematical modeling of turbulent mixing in compressed matters*): in 2 v. V. 2. Sarov; 2020. 407 p. (in Russ.). ISBN 978-5-9515-0458-6
44. Razin A.N. *Modelirovanie turbulentnogo peremeshivaniya v gazovykh sloikakh* (*The modeling of turbulent mixing in gas layers*). Sarov; 2020. 290 p. (in Russ.). ISBN 978-5-9515-0434-0
45. Lebo I.G., Obruchev I.V. The modeling of two-dimensional vortex flows in a cylindrical channel using parallel calculation on a supercomputer. *Russ. Technol. J.* 2022;10(1):60–67 (in Russ.). https://doi.org/10.32362/2500-316X-2022-10-1-60-67
46. Obenschain S., Lehmlerg R., Kehne D., et al. High-energy krypton-fluoride laser for inertial fusion. *Appl. Opt.* 2015;54(31):F103–F122. http://dx.doi.org/10.1364/AO.54.00F103
47. Sethian J., Obenschain S. Fusion energy with krypton fluoride lasers and direct drive targets. *Fusion Sci. Technol*. 2012;61(1T):41–46. https://doi.org/10.13182/FST12-A13394
48. Wolford M.F., Sethian J.D., Myers M.C., Hegeler F., Giuliani J.L., Obenschain S.P. Krypton fluoride (KrF) laser for inertial fusion energy. *Fusion Sci. Technol*. 2013;64(2):179–186. https://doi.org/10.13182/FST12-502
49. Bodner S.E. The path to electrical energy using laser fusion. *High Power Laser Science and Engineering.* 2019;7:e63. https://doi.org/10.1017/hpl.2019.51
50. Schmitt A.J., Obenschain S.P. The importance of laser wavelength for driving inertial confinement fusion targets. I. Basic physics. *Phys. Plasmas*. 2023;30(1):012701. https://doi.org/10.1063/5.0118080
51. Schmitt A.J., Obenschain S.P. The importance of laser wavelength for driving inertial confinement fusion targets. II. Target design. *Phys. Plasmas*. 2023;30(1):012702. https://doi.org/10.1063/5.0118093

## About the author

**Ivan G. Lebo,** Dr. Sci. (Phys.-Math.), Professor, Department of Higher Mathematics, Institute of Artificial Intelligence, MIREA – Russian Technological University (78, Vernadskogo pr., Moscow, 119454 Russia). E-mail: lebo@mirea.ru. RSCI SPIN-code 9416-5542, https://orcid.org/0000-0001-8341-9453

## Об авторе

**Лебо Иван Германович,** д.ф.-м.н., профессор, кафедра высшей математики Института искусственного интеллекта ФГБОУ ВО «МИРЭА – Российский технологический университет» (119454, Россия, Москва, пр-т Вернадского, д. 78). E-mail: lebo@mirea.ru. SPIN-код РИНЦ 9416-5542, https://orcid.org/0000-0001-8341-9453

*Translated from Russian into English by Kirill V. Nazarov*
*Edited for English language and spelling by Thomas A. Beavitt*